



# A Translational Regulatory Mechanism Mediated by Hypusinated Eukaryotic Initiation Factor 5A Facilitates $\beta$ -Cell Identity and Function

Craig T. Connors,<sup>1</sup> Catharina B.P. Villaca,<sup>1</sup> Emily K. Anderson-Baucum,<sup>2</sup> Spencer R. Rosario,<sup>3</sup> Caleb D. Rutan,<sup>1</sup> Paul J. Childress,<sup>2</sup> Leah R. Padgett,<sup>2</sup> Morgan A. Robertson,<sup>1</sup> and Teresa L. Mastracci<sup>1,4,5</sup>

*Diabetes* 2024;73:461–473 | <https://doi.org/10.2337/db23-0148>

As professional secretory cells,  $\beta$ -cells require adaptable mRNA translation to facilitate a rapid synthesis of proteins, including insulin, in response to changing metabolic cues. Specialized mRNA translation programs are essential drivers of cellular development and differentiation. However, in the pancreatic  $\beta$ -cell, the majority of factors identified to promote growth and development function primarily at the level of transcription. Therefore, despite its importance, the regulatory role of mRNA translation in the formation and maintenance of functional  $\beta$ -cells is not well defined. In this study, we have identified a translational regulatory mechanism mediated by the specialized mRNA translation factor eukaryotic initiation factor 5A (eIF5A), which facilitates the maintenance of  $\beta$ -cell identity and function. The mRNA translation function of eIF5A is only active when it is posttranslationally modified (“hypusinated”) by the enzyme deoxyhypusine synthase (DHPS). We have discovered that the absence of  $\beta$ -cell DHPS in mice reduces the synthesis of proteins critical to  $\beta$ -cell identity and function at the stage of  $\beta$ -cell maturation, leading to a rapid and reproducible onset of diabetes. Therefore, our work has revealed a gatekeeper of specialized mRNA translation that permits the  $\beta$ -cell, a metabolically responsive secretory cell, to maintain the integrity of protein synthesis necessary during times of induced or increased demand.

The pancreatic insulin-producing  $\beta$ -cell functions to maintain whole-body metabolism. As such,  $\beta$ -cells must have the capacity for high-level, adaptable mRNA translation to facilitate the rapid synthesis of proteins, including insulin, in response

## ARTICLE HIGHLIGHTS

- $\beta$ -Cells are secretory cells that require adaptable mRNA translation for the synthesis of proteins in response to metabolic cues. Our previous work showed that the hypusinated form of the mRNA translation factor eukaryotic initiation factor 5A (eIF5A<sup>HYP</sup>) translationally regulates acinar cell growth/function. We hypothesized this may also occur in  $\beta$ -cells.
- We discovered that *Ins1*, *Slc2a2* (Glut2), *Ucn3*, and *Chga* are translationally regulated by eIF5A<sup>HYP</sup> during  $\beta$ -cell maturation. Without deoxyhypusine synthase (DHPS)/eIF5A<sup>HYP</sup>,  $\beta$ -cells lose identity/function and diabetes ensues.
- Our findings suggest that secretory cells regulate translation during times of stress. We propose that stimulating translation in the  $\beta$ -cell might reverse defects that contribute to diabetes progression.

to changing metabolic cues (1,2). In other cellular settings, specialized mRNA translation programs have been shown to drive cellular development, differentiation, and function (3,4). However, most of the factors identified to promote growth and development in the pancreatic  $\beta$ -cell primarily function at the level of transcription (5). Therefore, despite its importance, the regulatory role of mRNA translation in the formation and maintenance of functional  $\beta$ -cells is not as thoroughly studied. If we are to

<sup>1</sup>Department of Biology, Indiana University Indianapolis, Indianapolis, IN

<sup>2</sup>Indiana Biosciences Research Institute, Indianapolis, IN

<sup>3</sup>Department of Biostatistics and Bioinformatics, Roswell Park Comprehensive Cancer Center, Buffalo, NY

<sup>4</sup>Department of Biochemistry and Molecular Biology, Indiana University School of Medicine, Indianapolis, IN

<sup>5</sup>Center for Diabetes and Metabolic Diseases, Indiana University School of Medicine, Indianapolis, IN

Corresponding author: Teresa L. Mastracci, [tmastrac@iu.edu](mailto:tmastrac@iu.edu)

Received 21 February 2023 and accepted 27 November 2023

This article contains supplementary material online at <https://doi.org/10.2337/figshare.24721620>.

C.T.C. and C.B.P.V. contributed equally to this work.

© 2024 by the American Diabetes Association. Readers may use this article as long as the work is properly cited, the use is educational and not for profit, and the work is not altered. More information is available at <https://www.diabetesjournals.org/journals/pages/license>.

successfully engineer regenerative therapeutics to prevent or treat diabetes, a disease characterized by loss or dysfunction of the insulin-producing  $\beta$ -cells, we must first understand all of the mechanisms that drive functional  $\beta$ -cell development (6).

The endogenous generation of functional  $\beta$ -cells involves a multistep and progressive developmental program. Many transcription factors, including Pdx1, Nkx6.1, Nkx2.2, and Neurod1, are essential for specifying  $\beta$ -cell fate during embryonic pancreas development (7). Additional maturation is then acquired in the postnatal period following the upregulation of several markers required for maintenance of cellular identity and function, including Slc2a2 (Glut2), Ucn3, and MafA (8–11). The expression of proteins needed for  $\beta$ -cell functional development is increased in a timed manner that follows with the progression of the animal through expansion of  $\beta$ -cell mass in the perinatal period and enhancement of secretory machinery function after weaning (12). Clearly, this well-regulated timeline requires coordination between transcriptional and translational machinery. However, the mechanisms regulated by mRNA translation are not completely understood.

An important regulator of mRNA translation is eukaryotic initiation factor 5A (eIF5A) (13,14). Genome-wide association studies have identified *Eif5a* in a type 1 diabetes (T1D) susceptibility locus in humans and NOD mice (15,16), and the eIF5A pathway was shown to be active in islets during T1D (17). These findings suggest that eIF5A is of great significance to the  $\beta$ -cell and that this translation factor may function to establish and/or maintain proper  $\beta$ -cell health (18). For eIF5A to perform its function in mRNA translation, it must be posttranslationally modified by the rate-limiting enzyme deoxyhypusine synthase (DHPS) in a process known as hypusine biosynthesis. DHPS catalyzes the addition of a 4-aminobutyl moiety from the polyamine spermidine on to the lysine at position 50 of eIF5A, which generates the modified amino acid hypusine (*N*-4-amino-2-hydroxybutyl(lysine)) and thus the hypusinated form of eIF5A (eIF5A<sup>HYP</sup>) (19). eIF5A has been shown to be the only protein hypusinated by DHPS (20,21). The eIF5A<sup>HYP</sup> form is considered the “active” form, and it functions in the cytoplasm to facilitate mRNA translation initiation, elongation, and termination (22–27). Genetic deletion of *Dhps*, and thus loss of eIF5A<sup>HYP</sup>, specifically in the embryonic pancreas, was shown to alter mRNA translation, with specific reductions in the synthesis of proteins critical for exocrine pancreas growth and function (28,29). Moreover, inducible loss of *Dhps* in the adult  $\beta$ -cell in the setting of a high-fat diet was shown to impair compensatory  $\beta$ -cell proliferation (30). Therefore, there is growing evidence that mRNA translation facilitated by DHPS/eIF5A<sup>HYP</sup> is a critical regulatory mechanism to produce and maintain function in secretory cells in the pancreas.

Herein, we generated a mouse model with a  $\beta$ -cell-specific deletion of *Dhps* from the onset of  $\beta$ -cell differentiation in the embryo to determine the role of DHPS/eIF5A<sup>HYP</sup> in  $\beta$ -cell development and function. Our findings

reveal that DHPS is dispensable for perinatal  $\beta$ -cell development; however, the active form of the specialized translation factor eIF5A regulates the synthesis of critical proteins, including insulin and Glut2, which are needed for postnatal  $\beta$ -cell identity and function.

## RESEARCH DESIGN AND METHODS

### Animal Studies

Animal studies were approved by the Indiana University School of Medicine Institutional Animal Care and Use Committee and the Indiana University-Purdue University Indianapolis School of Science Institutional Animal Care and Use Committee. Mice containing the *Dhps*<sup>LoxP</sup> allele (B6.Cg-Dhps<sup>tm1.1Mirm/J</sup>) (30) were mated with *Ins1-cre* mice (B6(Cg)-Ins1<sup>tm1.1(cre)Thor/J</sup>) (31) to generate mutants (*Dhps*<sup>LoxP/LoxP</sup>; *Ins1-cre*, denoted as DHPS <sup>$\Delta$ BETA</sup>) and littermate controls. Given that the *Ins1-cre* is a knock-in allele, all matings were arranged to produce only animals heterozygous for this allele. To provide a lineage trace and confirm cre-mediated recombination, the *R26R*<sup>Tomato</sup> reporter (B6.Cg-Gt(ROSA)26Sor<sup>tm14(CAG-tdTomato)Hze/J</sup>) (32) was bred into the mouse model. All animals were maintained on a C57Bl/6 background and genotyped as previously described (30–32).

### Metabolic Analyses

Animals were weaned at 3 weeks of age. From weaning until 6 weeks of age, body weight and blood glucose were measured weekly using a digital scale (Fisher Scientific) and AlphaTrak2 glucose monitor and test strips (ADW Diabetes), respectively. At 4 weeks of age, male and female animals were fasted for 5 h, and a glucose tolerance test (GTT) performed. For the GTT, animals were injected intraperitoneally with 2 g/kg glucose (0.25 g/mL stock solution; Fisher Scientific), and blood glucose was measured from tail blood at 0, 15, 30, 45, 60, 90, 120 min after injection. Statistical significance was determined using a one-way ANOVA (GraphPad Prism 9, version 9.5.1, GraphPad Software).

One-week-old animals were also evaluated for body weight and ad libitum-fed blood glucose measurements as described above. Blood was collected into EDTA-coated tubes (Fisher Scientific) and processed by centrifugation (2,000 relative centrifugal force, 5 min). Separate cohorts of animals at 4, 4.5, and 6 weeks of age were evaluated for blood glucose levels after a 5-h fast; blood was collected from tail vein (6 weeks of age) or by decapitation (1 and 4 weeks of age) into EDTA-coated tubes (Fisher Scientific) and processed as above. Plasma samples from animals at 1, 4, and 6 weeks of age were analyzed by ELISA for insulin (ALPCO) and glucagon content (Mercodia). Statistical significance was determined using a Student *t* test (GraphPad Prism 9, version 9.5.1, GraphPad Software).

### Immunofluorescence, Immunohistochemistry, and Morphometric Analysis

Pancreas tissue at 1, 4, and 6 weeks of age was fixed in 4% paraformaldehyde (Acros Organics), cryopreserved using



30% sucrose (Fisher Scientific), embedded in optimal cutting temperature compound (Fisher Scientific), and sectioned (8  $\mu\text{m}$ ) using a CM1950 Cryostat (Leica). For 1-week-old samples, every 10th section was evaluated across the entire pancreas totaling 6 of 60 sections; for 4- and 6-week-old pancreata, every 10th section was evaluated across the entire pancreas totaling 10 of 100 sections. Immunofluorescence was performed as previously described (33). Primary and secondary antibodies are listed in the Supplementary Materials (Supplementary Table 1). Whole-section tile scan and individual islet images were acquired using a 710 confocal microscope (Zeiss) or a C2 confocal microscope (Nikon Corporation). All islets were evaluated from every section imaged. For morphometric analysis, insulin and glucagon areas were measured across the entire tissue section and normalized to exocrine area as visualized by carboxypeptidase A. Zen Blue V2.3 software (Zeiss) was used to calculate endocrine and exocrine area. Islet area, shape (circularity and length), and proximity to ducts were measured using QuPath software (<https://qupath.github.io/>) (34). For cell counting analysis from 6-week-old tissue, islet z-stack images were evaluated using NIS Elements Software V5.30.01 (Nikon Corporation). All islets were evaluated from every section imaged. The islet cell populations counted included lineage-labeled  $\beta$ -cells (Tomato<sup>+</sup>/insulin<sup>+</sup>), lineage-labeled  $\beta$ -cells lacking insulin (Tomato<sup>+</sup>/insulin<sup>-</sup>), and  $\beta$ -cells lacking the lineage label (Tomato<sup>-</sup>/insulin<sup>+</sup>). Within the Tomato-expressing population, cells were also counted for expression of  $\beta$ -cell identity and function markers, including Glut2, Pdx1, and MafA; total cell counts were graphed. For cell counting analyses from 1-week-old tissue, insulin and glucagon single and coexpressing cell populations were evaluated and graphed as a percentage. Additionally, islet and duct structures were measured from 1-week-old tissue using the pixel classifier, and distance between structures was measured from the center of each islet to the nearest duct. Statistical significance was determined using a Student *t* test (GraphPad Prism 9, version 9.5.1, GraphPad Software).

Immunohistochemistry was also used for morphometric analysis of pancreas tissue from 4- and 6-week-old animals. Briefly, tissue sections were washed in 0.3% hydrogen peroxide in PBS (both Fisher Scientific). Tissue sections were then permeabilized in PBS with 0.1% TritonX (Fisher Scientific) and blocked with 5% donkey serum in PBS. Primary and secondary antibodies are listed in Supplementary Materials (Supplementary Table 1). Tissue sections were developed in 3,3'-diaminobenzidine solution (Fisher Scientific) for 10 min. Hematoxylin (Sigma-Aldrich) was used as a counterstain to visualize tissue architecture. All sections were rinsed in water and dehydrated in ethanol (Decon Laboratories), cleared in xylene (Fisher Scientific), and mounted using Permount (Fisher Scientific). Insulin or glucagon area was normalized to total pancreas area. Zen Blue V2.3 software (Zeiss) was used to calculate endocrine and exocrine. Statistical significance was determined using a

Student *t* test (GraphPad Prism 9, version 9.5.1, GraphPad Software).

### TUNEL Analysis

Pancreas tissue from 5-week-old mice was harvested, cryopreserved, and sectioned as described above. The TUNEL assay was performed using the Invitrogen Click-iT Plus TUNEL Assay Kit for In Situ Apoptosis Detection (C10617, Invitrogen) according to the manufacturer's instructions. Briefly, tissue sections were permeabilized using proteinase K, followed by incubation in the terminal deoxynucleotidyl transferase reagent for 60 min at 37°C. The slides were washed and incubated with the Click-iT reaction cocktail for 30 min at 37°C. The slides were then stained for insulin, as described above. Primary and secondary antibodies are listed in Supplementary Table 1. Pancreas tissue sections treated with DNase were used as the positive control (TUNEL control) for every round of staining to ensure TUNEL assay acuity. Individual islet z-stack images were acquired using a C2 confocal microscope (Nikon Corporation). All islets were evaluated from every section imaged. For identifying positive nuclei, islet z-stack images were analyzed using NIS Elements Software V5.30.01 (Nikon Corporation). TUNEL-positive nuclei were identified within each population of  $\beta$ -cells. Statistical significance was determined using a Student *t* test (GraphPad Prism 9, version 9.5.1, GraphPad Software).

### Western Blot Analysis

Pancreatic islets were isolated from mice at 4 weeks of age (35) (see Supplementary Materials) and evaluated by Western blot analysis, as previously described (28). Primary and secondary antibodies are listed in Supplementary Table 1. After incubation with secondary antibodies, membranes were washed with 1% Tween (Fisher Scientific) in PBS and then imaged and quantified by densitometry using Image Studio Software (LICOR Biosciences). Densitometric data are graphed as relative expression. Statistical significance was determined using a Student *t* test (GraphPad Prism 9, version 9.5.1, GraphPad Software).

### Quantitative Mass Spectrometry and Proteomic Data Analysis

Pancreatic islets were isolated from mice at 4 weeks of age (see Supplementary Materials) and subjected to proteomic analysis by mass spectrometry. Islets were collected from *Dhps*<sup>loxP/loxP</sup>; *Ins1-cre*; *R26R*<sup>Tomato</sup>, and *Ins1-cre*; *R26R*<sup>Tomato</sup> mice. There were 116 to 193 islets per sample. Sample preparation and mass spectrometry analysis was performed in collaboration with the Indiana University Center for Proteome Analysis at the Indiana University School of Medicine, as previously published (28). Specific details for islet sample preparation, peptide measurement by mass spectrometry, and data analysis are in the Supplementary Materials.

Differentially expressed proteins (DEPs) were deemed significant with a  $|\log \text{ fold change [FC]}| > 1.5$  and  $P < 0.05$ . DEPs were then functionally enriched using the STRING

database (36) to assess relationships between proteins, generate a network, and enrich for pathways in which differential proteins appear (37). The Wikipathways 3.3.7 (38) plug-in for Cytoscape 3.8.2 (39) was used to integrate and visualize functionally enriched pathways of interest based on protein-level expression. The analysis was performed in the R 4.0.1 environment for statistical computing.

### Real-Time PCR

Real-time PCR was performed as previously described (40). Briefly, we isolated islets from 4-week-old mice (see Supplementary Materials) and extracted RNA using the RNeasy Micro Kit (QIAGEN). Total RNA was reverse transcribed using the High-Capacity cDNA Reverse Transcription Kit (Fisher Scientific). Real-time PCR was performed using TaqMan Gene Expression Master Mix (Applied Biosystems) and TaqMan probes for *Ins1*, *Slc2a2*, *Chga*, *Ucn3*, *Pdx1*, *Mafa*, and *Luciferase*. Gene expression was normalized by a spike-in *Luciferase* RNA (1  $\mu\text{g}/\mu\text{L}$ ). The mRNA abundance was graphed as relative expression, and statistical significance was determined using a Student *t* test (GraphPad Prism 9, version 9.5.1, GraphPad Software).

### Data and Resource Availability

The raw and processed mass spectrometry data generated during the current study are available in the Mass Spectrometry Interactive Virtual Environment (MassIVE) repository, a member of ProteomeXchange (accession ID MSV000093089). No applicable resources were generated or analyzed during the current study.

## RESULTS

### *Dhps* Is Dispensable for Perinatal $\beta$ -Cell Development

Our previous work defined a role for DHPS/eIF5A<sup>HYP</sup> in exocrine pancreas development and function (28). However, the extreme exocrine pancreas loss and reduced postnatal survival of the DHPS <sup>$\Delta$ PANC</sup> mouse model (28) precluded further examination of  $\beta$ -cell growth, maturation, and function. Therefore, to determine the role of DHPS specifically in the  $\beta$ -cell, we generated a mouse model with a genetic deletion of *Dhps* in the insulin-expressing cells from the onset of  $\beta$ -cell differentiation in the embryo (*Dhps*<sup>*LoxP/LoxP*</sup>; *Ins1-cre*; *R26R*<sup>*Tomato*</sup>, denoted DHPS <sup>$\Delta$ BETA</sup>) (Fig. 1A–E). DHPS <sup>$\Delta$ BETA</sup> mutant animals were viable, and Western blot analysis of isolated islets confirmed knockdown of DHPS concomitant with a significant reduction in eIF5A<sup>HYP</sup> (Fig. 1F–I).

Morphometric analysis was performed on pancreas tissue collected from DHPS <sup>$\Delta$ BETA</sup> animals and *Ins1-cre* controls during two significant time points in the life of the  $\beta$ -cell: 1) the first week of life (postnatal day 7), which is during a stage of significant  $\beta$ -cell growth (up to postnatal day 15) (41), and 2) weaning, which is characterized by  $\beta$ -cell functional maturation (12,42,43).  $\beta$ -cell area in 1-week-old DHPS <sup>$\Delta$ BETA</sup> mice and *Ins1-cre* controls was evaluated by immunofluorescence. Insulin-expressing  $\beta$ -cells and glucagon-expressing  $\alpha$ -cells were visualized, and quantification

showed no significant difference in  $\beta$ -cell area, insulin- or glucagon-expressing cell number, insulin/glucagon coexpressing cell number, islet size, or islet architecture between DHPS <sup>$\Delta$ BETA</sup> mice and *Ins1-cre* controls (Fig. 1J–L and Supplementary Fig. 1). Body weight and ad libitum fed blood glucose, plasma insulin, and glucagon levels were also not significantly different between DHPS <sup>$\Delta$ BETA</sup> and controls at this time point (Fig. 1M–P). Altogether, these data identify that the absence of *Dhps* in the  $\beta$ -cell does not impact perinatal  $\beta$ -cell growth, islet architecture, or whole-body metabolism, suggesting that *Dhps* is dispensable for early postnatal  $\beta$ -cell growth and function.

### Deletion of $\beta$ -cell *Dhps* Results in the Onset of Diabetes After Weaning

The functional maturation of  $\beta$ -cells occurs around weaning age (3–4 weeks of age). At this stage, animals experience a change in nutrition, and their  $\beta$ -cells undergo a maturation that includes the acquisition of glucose-stimulated insulin secretion (12). Therefore, we assessed DHPS <sup>$\Delta$ BETA</sup> and *Ins1-cre* mice for changes in metabolic parameters at this stage of  $\beta$ -cell development. Animals were evaluated beginning at 3 weeks of age, and we observed no significant difference in body weight between DHPS <sup>$\Delta$ BETA</sup> and *Ins1-cre* animals until 6 weeks of age (Fig. 2A). Whereas GTTs at 4 weeks of age showed a normal glucose response (Fig. 2B and C), DHPS <sup>$\Delta$ BETA</sup> mice dramatically progressed to hyperglycemia and then overt diabetes by 6 weeks of age (mean blood glucose of 675 mg/dL in males) (Fig. 2D). Fasted blood glucose levels also confirmed the progression to diabetes, as DHPS <sup>$\Delta$ BETA</sup> mice displayed elevated fasting blood glucose levels beginning at 4.5 weeks of age (mean blood glucose of 370 mg/dL in males), with an even greater defect observed at 6 weeks of age (mean blood glucose of 576 mg/dL in males) (Fig. 2E). Male and female DHPS <sup>$\Delta$ BETA</sup> and *Ins1-cre* mice were evaluated at all time points, and identical phenotypes were observed in both sexes (Fig. 2F–J). These data identify that *Dhps* plays a critical role in postnatal  $\beta$ -cell function.

### $\beta$ -Cells in DHPS <sup>$\Delta$ BETA</sup> Mice Have Reduced Insulin Expression After 4 Weeks of Age

We showed that DHPS <sup>$\Delta$ BETA</sup> mice develop hyperglycemia and diabetes after weaning. To determine the  $\beta$ -cell defect that contributes to this phenotype, we first performed morphometric analysis of pancreas tissue from DHPS <sup>$\Delta$ BETA</sup> and *Ins1-cre* animals at 4 weeks of age, using immunohistochemistry to identify the insulin-expressing cells. Similar to what we observed at 1 week of age, islet structure at 4 weeks of age was not changed between the DHPS <sup>$\Delta$ BETA</sup> mutants and *Ins1-cre* controls (Fig. 3A and B), and quantification of insulin area showed no significant difference (Fig. 3C). Moreover, DHPS <sup>$\Delta$ BETA</sup> and *Ins1-cre* mice at 4 weeks of age showed no difference in levels of plasma insulin or glucagon (Fig. 3D and Supplementary Fig. 2A). These results are in line with the normal GTTs

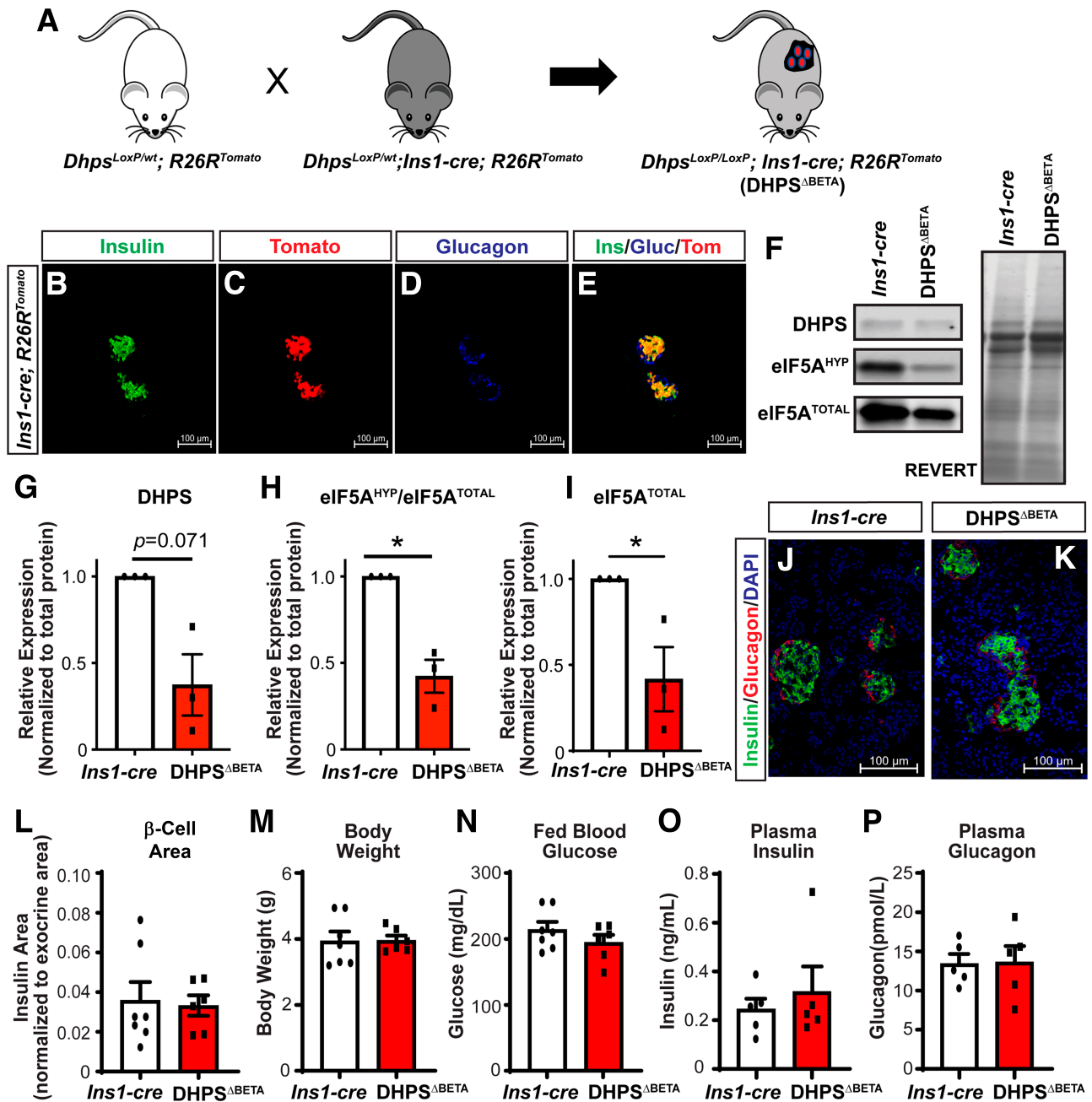


**Figure 1**—A mouse model of  $\beta$ -cell-specific genetic deletion of *Dhps* (DHPS<sup>ΔBETA</sup>). **A**: Mouse alleles used to generate the  $\beta$ -cell-specific deletion of *Dhps* (DHPS<sup>ΔBETA</sup>). Pancreas tissue from control animals (*Ins1-cre*; *R26R<sup>Tomato</sup>*) was evaluated by immunofluorescence for expression of insulin (**B**), Tomato (**C**), and glucagon (**D**) to confirm  $\beta$ -cell-specific Cre activity. **E**: Islets show coexpression of Tomato in the insulin-expressing  $\beta$ -cells. **F**: Western blot analysis of islets from 4-week-old DHPS<sup>ΔBETA</sup> mutants for expression of DHPS, eIF5A<sup>HYP</sup>, eIF5A<sup>TOTAL</sup>, and total protein (as visualized by Revert). Densitometric data for DHPS (**G**), the ratio of eIF5A<sup>HYP</sup>-to-eIF5A<sup>TOTAL</sup> (**H**), and total eIF5A ( $n = 3$ /group) (**I**). Immunofluorescence to visualize insulin, glucagon, and DAPI was performed on pancreata from 1-week-old *Ins1-cre* (**J**) and DHPS<sup>ΔBETA</sup> mice (**K**). **L**: Quantification of  $\beta$ -cell area ( $n = 6$ – $7$ /group). Body weight (**M**) and ad libitum fed blood glucose levels (**N**) at 1 week of age ( $n = 6$ – $7$ /group). Plasma insulin (**O**) and glucagon (**P**) levels were measured ( $n = 5$ – $7$ /group). Quantitative data are represented as mean  $\pm$  SEM. \* $P < 0.05$ . Scale bar: 100  $\mu$ m.

and fasted blood glucose levels observed at 4 weeks of age in the DHPS<sup>ΔBETA</sup> mice (Fig. 2B, C, E, G, H, and J).

Because DHPS<sup>ΔBETA</sup> mice were metabolically healthy at 4 weeks of age but rapidly progressed to diabetes two weeks later, we examined pancreas tissue from DHPS<sup>ΔBETA</sup> and *Ins1-cre* mice at 6 weeks of age. Using morphometric analysis

and insulin expression to identify the  $\beta$ -cells, we observed a significant reduction in the insulin-expressing cell area in the DHPS<sup>ΔBETA</sup> compared with *Ins1-cre* mice (Fig. 3E–G). Concomitant with a reduction of insulin-expressing cells, plasma insulin was reduced in DHPS<sup>ΔBETA</sup> mice compared with *Ins1-cre* controls (Fig. 3H). This change in insulin-expressing

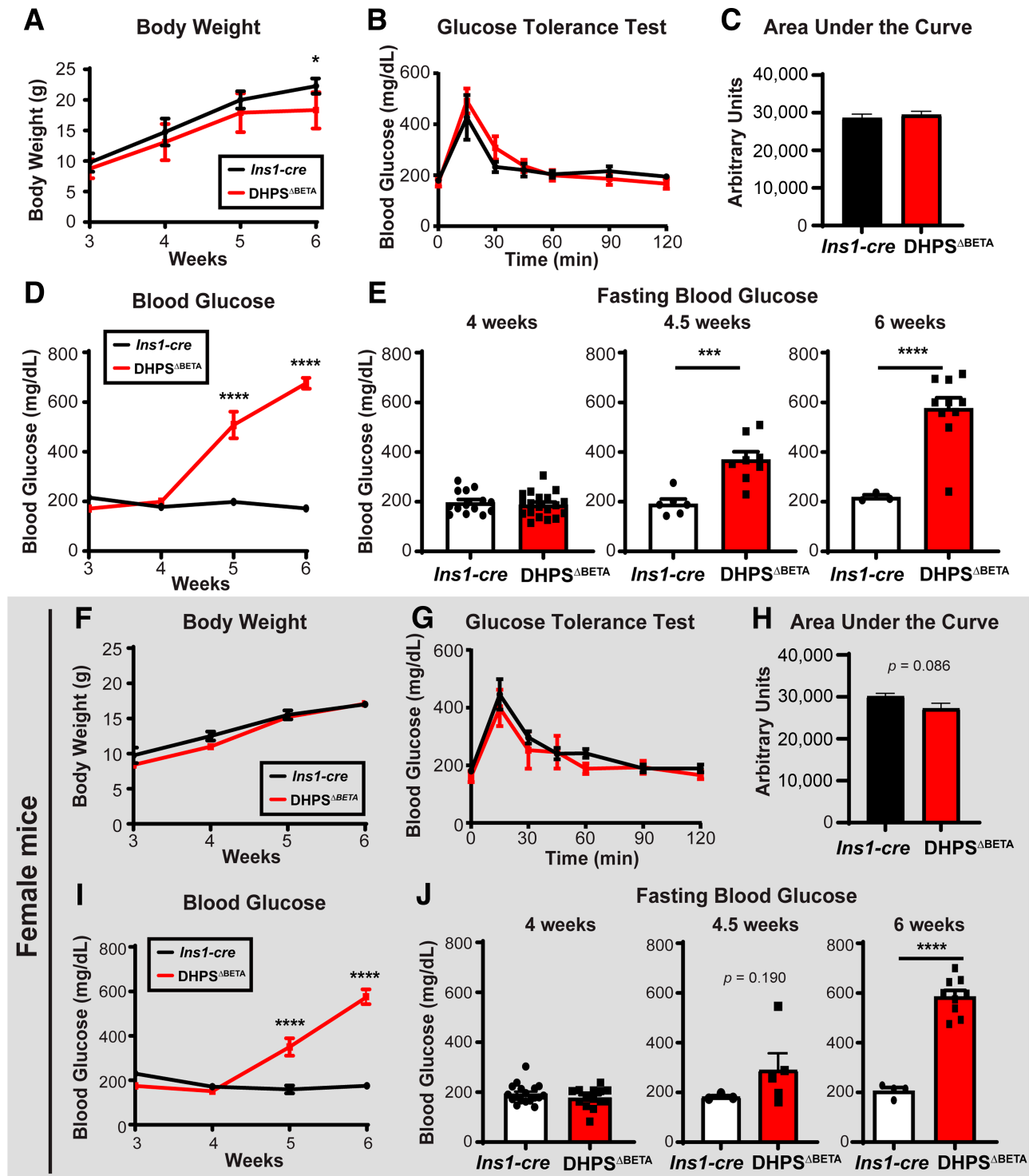


**Figure 2—**Measurement of metabolic parameters in the  $DHPS^{\Delta BETA}$  mice after weaning. **A:** Body weight in male mice was measured in  $Ins1-cre$  and  $DHPS^{\Delta BETA}$  mice weekly beginning at weaning (3 weeks;  $n = 4-8$ /group). **B:** GTTs were performed on 4-week-old mice ( $n = 4-8$ /group). **C:** Area under the curve was quantified from GTT data. **D:** Blood glucose was measured weekly beginning at weaning ( $n = 4-8$ /group). **E:** Blood glucose was measured after a 5-h fast in 4-, 4.5-, and 6-week-old mice ( $n = 3-19$ /group). **F–J:** The identical phenotype was observed in female mice for all parameters. Quantitative data are represented as mean  $\pm$  SEM. \* $P < 0.05$ ; \*\*\* $P < 0.001$ ; \*\*\*\* $P < 0.0001$ .

cell area and function did not impact the  $\alpha$ -cells, as the  $DHPS^{\Delta BETA}$  mutants showed normal glucagon-expressing cell area and no change in plasma glucagon (Supplementary

Fig. 2B–E). All analyses were performed in both male and female  $DHPS^{\Delta BETA}$  and  $Ins1-cre$  mice, and identical phenotypes were observed (Fig. 3I–L).

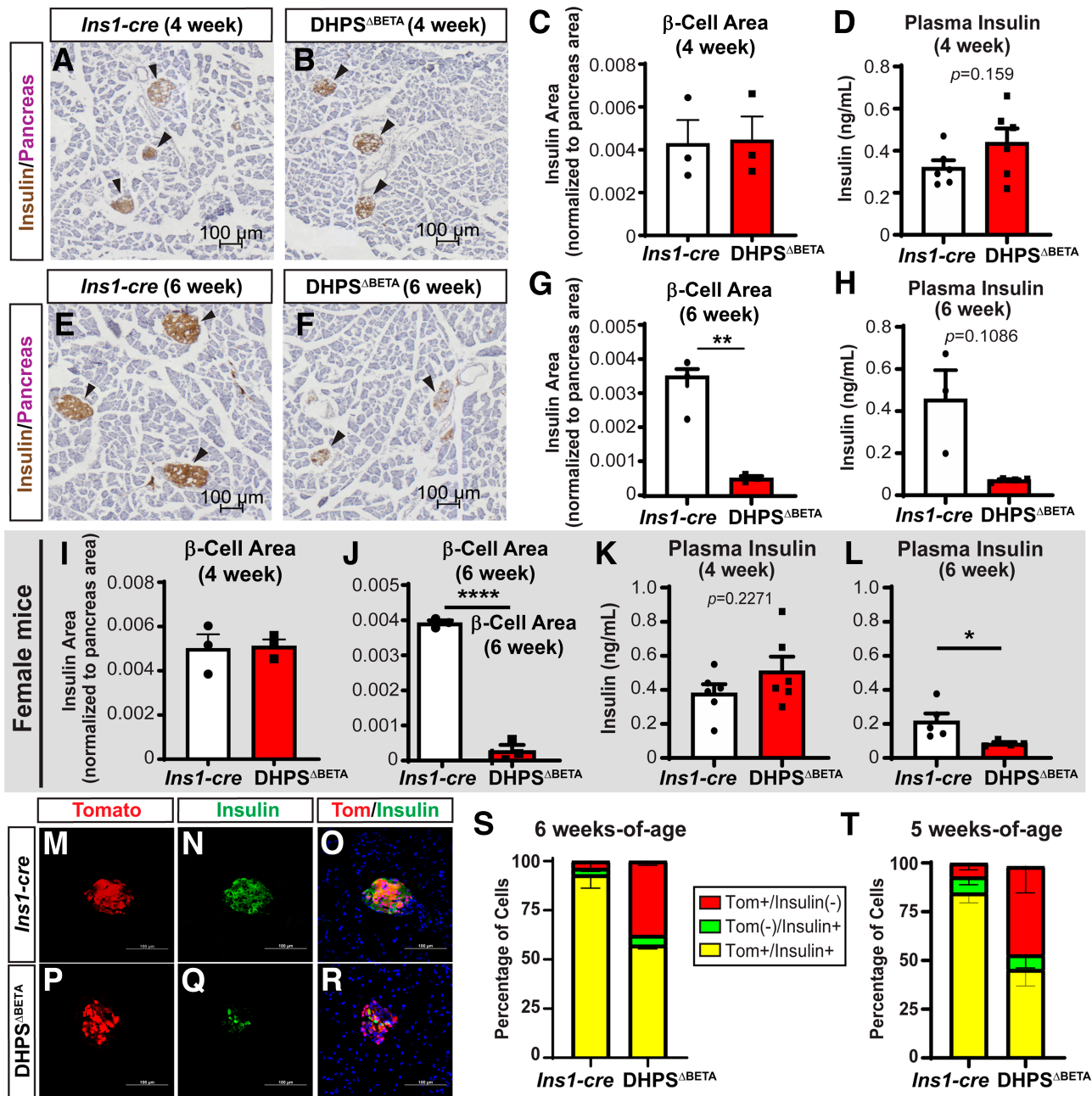


**Figure 3**—Insulin-expressing cell area in the *DHPS<sup>ΔBETA</sup>* mice is reduced at 5 and 6 weeks of age. Insulin expression in pancreas from 4-week-old *Ins1-cre* (A) and *DHPS<sup>ΔBETA</sup>* (B) mice. Eosin (purple) defines pancreas area. C: β-Cell area normalized to pancreas area. D: Plasma insulin levels in 4-week-old *Ins1-cre* and *DHPS<sup>ΔBETA</sup>* mice ( $n = 6$ /group). Insulin expression in pancreas from 6-week-old *Ins1-cre* (E) and *DHPS<sup>ΔBETA</sup>* (F) mice ( $n = 3$ /group). Eosin (purple) defines pancreas area. G: β-Cell area normalized to pancreas area. H: Plasma insulin levels in 6-week-old *Ins1-cre* and *DHPS<sup>ΔBETA</sup>* mice ( $n = 3$ –4/group). I–L: Female mice show the same phenotype as male mice. Pancreas tissue from 6-week-old *Ins1-cre* (M–O) and *DHPS<sup>ΔBETA</sup>* (P–R) mice showing expression of insulin and the β-cell lineage reporter (Tomato) ( $n = 3$ /group). Scale bar: 100 μm. S: Tomato<sup>+</sup>/*Insulin*<sup>-</sup>, Tomato<sup>-</sup>/*Insulin*<sup>+</sup>, and Tomato<sup>+</sup>/*Insulin*<sup>+</sup> cell populations were quantified and expressed as the percentage of Tomato<sup>+</sup> cells (average Tomato<sup>+</sup> cell count: *Ins1-cre*, 7,475; *DHPS<sup>ΔBETA</sup>*, 5,517). T: Tomato<sup>+</sup>/*Insulin*<sup>-</sup>, Tomato<sup>-</sup>/*Insulin*<sup>+</sup>, and Tomato<sup>+</sup>/*Insulin*<sup>+</sup> cell populations were quantified in control and mutant mice at 5 weeks of age and expressed as the percentage of Tomato<sup>+</sup> cells (average Tomato<sup>+</sup> cell count: *Ins1-cre*, 10,422; *DHPS<sup>ΔBETA</sup>*, 12,934). Quantitative data are represented as mean ± SEM. \* $P < 0.05$ , \*\* $P < 0.01$ , \*\*\*\* $P < 0.0001$ .

Given that β-cell area was normal in *DHPS<sup>ΔBETA</sup>* mice at 4 weeks of age, the change in insulin-expressing cell area at 6 weeks of age could reflect that insulin synthesis was lost in the β-cells or that β-cell death occurred during that two-week time period. To address the first possibility,

we used the *R26R<sup>Tomato</sup>* reporter allele to lineage-label the β-cells and then determine whether insulin expression was lost in the *DHPS<sup>ΔBETA</sup>* mutant β-cells. Whole-mount imaging confirmed the presence of Tomato-expressing cells in isolated islets from both the *Ins1-cre* and *DHPS<sup>ΔBETA</sup>* mice



(Supplementary Fig. 3). However, morphometric analysis of pancreas tissue from 6-week-old animals revealed an unexpected and significant population of cells in the mutant islets that were  $R26R^{Tomato}$  lineage-positive but lacked insulin expression (Fig. 3M–S). Altogether we identified three populations of  $\beta$ -cells in the mutant islets: 1) insulin-expressing/ $R26R^{Tomato}$ -expressing  $\beta$ -cells, 2) insulin-deficient/ $R26R^{Tomato}$ -expressing  $\beta$ -cells, and 3) insulin-expressing  $\beta$ -cells that lacked the  $R26R^{Tomato}$  lineage label. By comparison, nearly all  $\beta$ -cells in *Ins1-cre* control islets coexpressed insulin and the  $R26R^{Tomato}$  lineage label, with only a small number of insulin-deficient/ $R26R^{Tomato}$ -expressing  $\beta$ -cells and insulin-expressing  $\beta$ -cells that lacked  $R26R^{Tomato}$  lineage label (Fig. 3S).

Given the significant increase in lineage-labeled  $\beta$ -cells that lacked insulin expression at 6 weeks of age, we collected pancreas tissue from a cohort of 5-week-old *Ins1-cre* and  $DHPS^{\Delta BETA}$  mice that also carried the  $R26R^{Tomato}$  reporter allele to determine whether there was evidence of apoptosis of the lineage-labeled  $\beta$ -cell populations. Using morphometric analysis, we identified that the same three populations of  $\beta$ -cells observed at 6 weeks of age were also present in similar proportions at 5 weeks of age in the  $DHPS^{\Delta BETA}$  mice (Fig. 3T). Stratifying the lineage labeled

(Tomato-expressing) cell populations by expression of insulin (Fig. 4A–I), we observed no difference in TUNEL-positive cells in the insulin-deficient/ $R26R^{Tomato}$ -expressing cells (Fig. 4J) or the insulin-expressing/ $R26R^{Tomato}$ -expressing cells (Fig. 4K). Altogether, our data confirm that after 4 weeks of age, the absence of *Dhps* in the  $\beta$ -cell does not induce  $\beta$ -cell death but does result in a loss of insulin-expressing  $\beta$ -cells.

### $\beta$ -Cells Require DHPS to Acquire Cellular Identity and Maturation

DHPS is the rate-limiting enzyme required for the hypusination of eIF5A, which is the process by which eIF5A becomes posttranslationally modified and thus active. The hypusinated/active form of eIF5A, eIF5A<sup>HYP</sup>, functions in specialized mRNA translation; however, the proteins that specifically require eIF5A<sup>HYP</sup> for their synthesis in the  $\beta$ -cell have not been identified. We speculated that the phenotype of diabetes in  $DHPS^{\Delta BETA}$  mice may be a result of altered specialized mRNA translation causing changes in the synthesis of certain critical  $\beta$ -cell proteins. Therefore, we performed quantitative mass spectrometry on isolated islets from 4-week-old *Ins1-cre* controls and  $DHPS^{\Delta BETA}$  mutants. Importantly, this time point is a stage when we

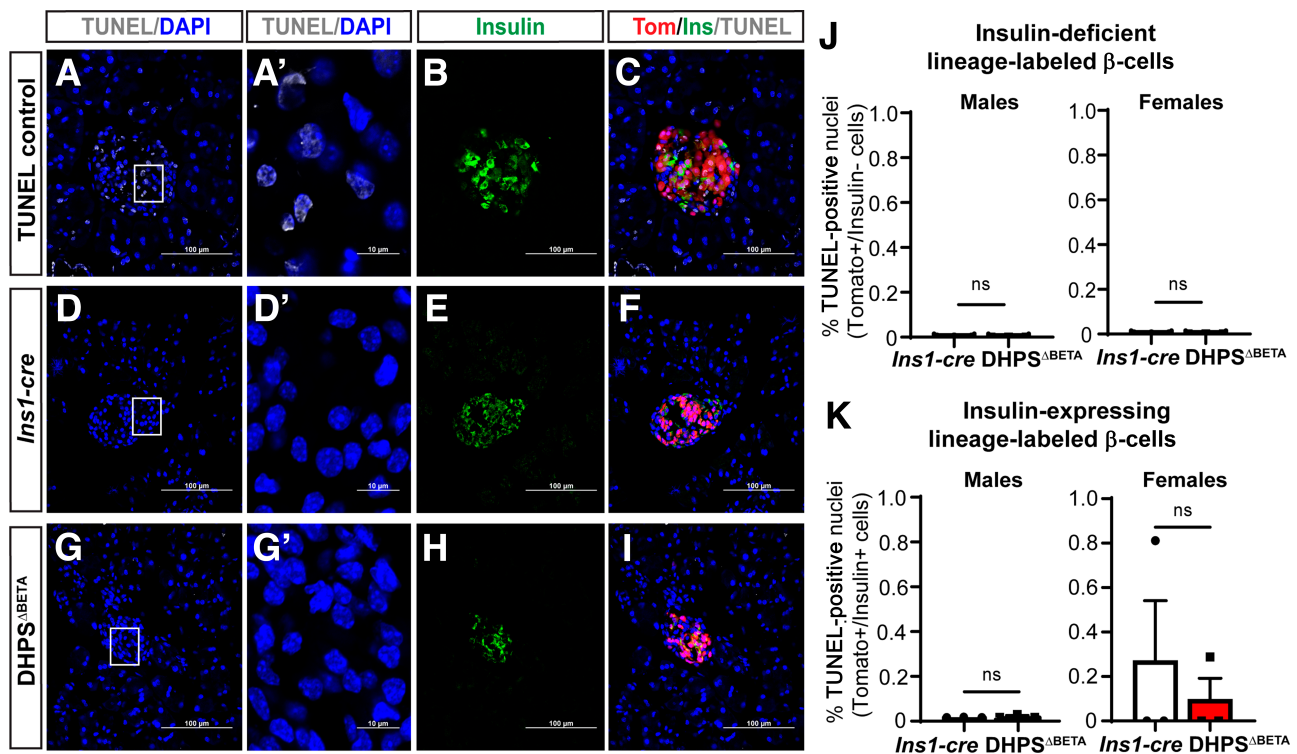


**Figure 4**— $\beta$ -Cell death is not observed in islets from  $DHPS^{\Delta BETA}$  mice. TUNEL assay was performed on pancreas tissue from 5-week-old TUNEL-positive control (tissue treated with DNase) (A–C), *Ins1-cre* (D–F), and  $DHPS^{\Delta BETA}$  (G–I) mice to determine cell death (TUNEL, white). Scale bar: 100  $\mu$ m. A', D', and G': Higher magnification to visualize location of TUNEL. Scale bar: 10  $\mu$ m. J: TUNEL<sup>+</sup> insulin-deficient lineage-labeled (Tomato<sup>+</sup>)  $\beta$ -cells were counted (average TUNEL<sup>+</sup> cells/insulin<sup>−</sup>Tomato<sup>+</sup> cells: *Ins1-cre* males, 0/8,624;  $DHPS^{\Delta BETA}$  males, 0/2,929; *Ins1-cre* females, 2.6/8,624;  $DHPS^{\Delta BETA}$  females, 2.5/11,120). K: TUNEL<sup>+</sup> insulin-expressing lineage-labeled (Tomato<sup>+</sup>)  $\beta$ -cells were counted (average TUNEL<sup>+</sup> cells/insulin<sup>+</sup>Tomato<sup>+</sup> cells: *Ins1-cre* males, 0/5,945;  $DHPS^{\Delta BETA}$  males, 0/9,489; *Ins1-cre* females, 0.6/3,782;  $DHPS^{\Delta BETA}$  females, 0/7,109) ( $n = 3$ /group). Data are represented as mean  $\pm$  SEM. ns, not significant.



observed no changes in insulin-expressing  $\beta$ -cell area or function. Therefore, this analysis will determine, in an unbiased manner, the proteins whose synthesis is altered in the absence of *Dhps* in the  $\beta$ -cell. Overall, proteomic analysis detected 5,900 proteins, with 123 significantly differentially expressed proteins ( $P < 0.05$ ;  $|\log_{2}FC| > 1.5$ ), both up- and downregulated, in the islets from DHPS<sup>ΔBETA</sup> mice compared with *Ins1-cre* controls. Pathway analysis revealed alterations in numerous pathways critical for  $\beta$ -cell function, including protein localization to the secretory granule, regulation of mRNA processing, and regulation of the cell cycle (Fig. 5A).

Given the observation that DHPS<sup>ΔBETA</sup> mutant islets contained a large population of insulin-deficient lineage-labeled  $\beta$ -cells by 6 weeks of age, we speculated that eIF5A<sup>HYP</sup> may regulate the translation of genes, including insulin, whose synthesis is increased during the stage of  $\beta$ -cell maturation. Excitingly, detailed examination of our proteomic data revealed that critical  $\beta$ -cell proteins were downregulated in the DHPS<sup>ΔBETA</sup> islets, including those involved in  $\beta$ -cell identity and function (Fig. 5B). Of particular significance, insulin (*Ins1*), glucose transporter 2 (*Slc2a2*), urocortin 3 (*Ucn3*), and chromogranin A (*Chga*) and were reduced in DHPS<sup>ΔBETA</sup> islets compared with *Ins1-cre* controls. To determine whether the synthesis of these proteins is translationally regulated, we examined RNA from 4-week-old *Ins1-cre* and DHPS<sup>ΔBETA</sup> islets to determine whether transcript levels were altered. We found that gene expression of *Ins1*, *Slc2a2*, *Ucn3*, and *Chga* was equivalent between the DHPS<sup>ΔBETA</sup> and *Ins1-cre* islets (Fig. 5C–F), confirming that the reduced protein synthesis was due to altered eIF5A<sup>HYP</sup>-mediated translational regulation. Moreover, these findings demonstrate that DHPS/eIF5A<sup>HYP</sup> regulates the synthesis of at least four proteins that impart cellular identity and function at the stage of  $\beta$ -cell maturation.

To directly connect the downregulated synthesis of essential  $\beta$ -cell proteins at 4 weeks of age (Fig. 5A–F) with the altered insulin secretion we observe at 6 weeks of age in the DHPS<sup>ΔBETA</sup> mice, we further evaluated *Glut2* expression, a transporter whose abundance and localization is essential for proper  $\beta$ -cell function. Therefore at 6 weeks of age, we performed morphometric analysis to visualize and quantify the change in protein expression. Immunofluorescence analysis showed punctate, intracellular expression of *Glut2* in DHPS<sup>ΔBETA</sup> lineage-labeled  $\beta$ -cells compared with membrane-bound expression of *Glut2* in *Ins1-cre* lineage-labeled  $\beta$ -cells (Fig. 5G–J). Furthermore, quantitative image analysis determined that the lineage-labeled (Tomato-expressing), insulin-deficient  $\beta$ -cells in the DHPS<sup>ΔBETA</sup> mutants were deficient in *Glut2* (Fig. 5K). These data corroborate our findings at 4 weeks of age and suggest that in addition to impaired  $\beta$ -cell maturation and function due to reduced synthesis of insulin and *Glut2*, altered protein localization can contribute to the

secretory vesicle and intracellular transport impairment identified in our proteomics (Fig. 5A and B).

As further evidence that  $\beta$ -cell maturation is altered in the absence of DHPS/eIF5A<sup>HYP</sup>, we examined islets from DHPS<sup>ΔBETA</sup> and *Ins1-cre* mice at 6 weeks of age for additional known markers of identity, namely, the transcription factors *Pdx1* and *MafA*. Similar to the evaluation of *Glut2*, we visualized cellular location and quantified expression of *Pdx1* and *MafA* by immunofluorescence. We observed that the insulin-deficient lineage-labeled (Tomato-expressing)  $\beta$ -cells in the DHPS<sup>ΔBETA</sup> mutants showed little or no *Pdx1* (Fig. 6A–D) or *MafA* (Fig. 6E–H). Quantification of this population of insulin-deficient lineage-labeled  $\beta$ -cells that lack critical transcription factor expression confirmed our observations (Fig. 6I and J). Interestingly, gene expression analysis of *Pdx1* and *Mafa* revealed that these transcripts were reduced (Fig. 6K and L). Altogether our data suggest that DHPS/eIF5A<sup>HYP</sup> facilitates a critical switch in the  $\beta$ -cell that drives the synthesis of proteins, including insulin and *Glut2*, that are needed for maturation. When this translational regulation mechanism is altered (through loss of DHPS/eIF5A<sup>HYP</sup>), defects in  $\beta$ -cell identity and function ensue.

## DISCUSSION

Identifying mechanisms that drive  $\beta$ -cell growth or cause  $\beta$ -cell dysfunction are paramount to developing therapeutics for diabetes. The treatment of diabetes currently involves the use of exogenous insulin and pharmacological intervention; however,  $\beta$ -cell replacement or regeneration would represent a step toward the restoration of  $\beta$ -cell mass and function. The development of such cellular therapeutics requires a detailed understanding of the mechanisms controlling the development of the  $\beta$ -cell throughout all stages of its life. In this study, we have identified that there exists a translational regulatory mechanism in the  $\beta$ -cell, driven by DHPS/eIF5A<sup>HYP</sup>, that facilitates the maintenance of  $\beta$ -cell maturation. Specifically, we have shown that  $\beta$ -cell-specific deletion of *Dhps* reduces the synthesis of proteins critical for  $\beta$ -cell identity and function at the stage of  $\beta$ -cell maturation. Furthermore, we have shown that when this translational regulatory mechanism is altered, there is a rapid and reproducible onset of diabetes.

To fully understand how  $\beta$ -cells develop, these cells must be studied at all stages of significant development in mice—from differentiation in the embryo, to expansion during the first 2 weeks of postnatal life, to functional maturation around weaning. In our previous work, we characterized a pancreas-specific deletion of *Dhps* (DHPS<sup>ΔPANC</sup>), which showed exocrine insufficiency but no change in  $\beta$ -cell differentiation or abundance in the embryo (28). In the current study, we observed proper perinatal  $\beta$ -cell growth and function in the DHPS<sup>ΔBETA</sup> mice but reduced identity and function after weaning. Therefore, our data demonstrate that embryonic and perinatal  $\beta$ -cells do not require the specialized translational regulation

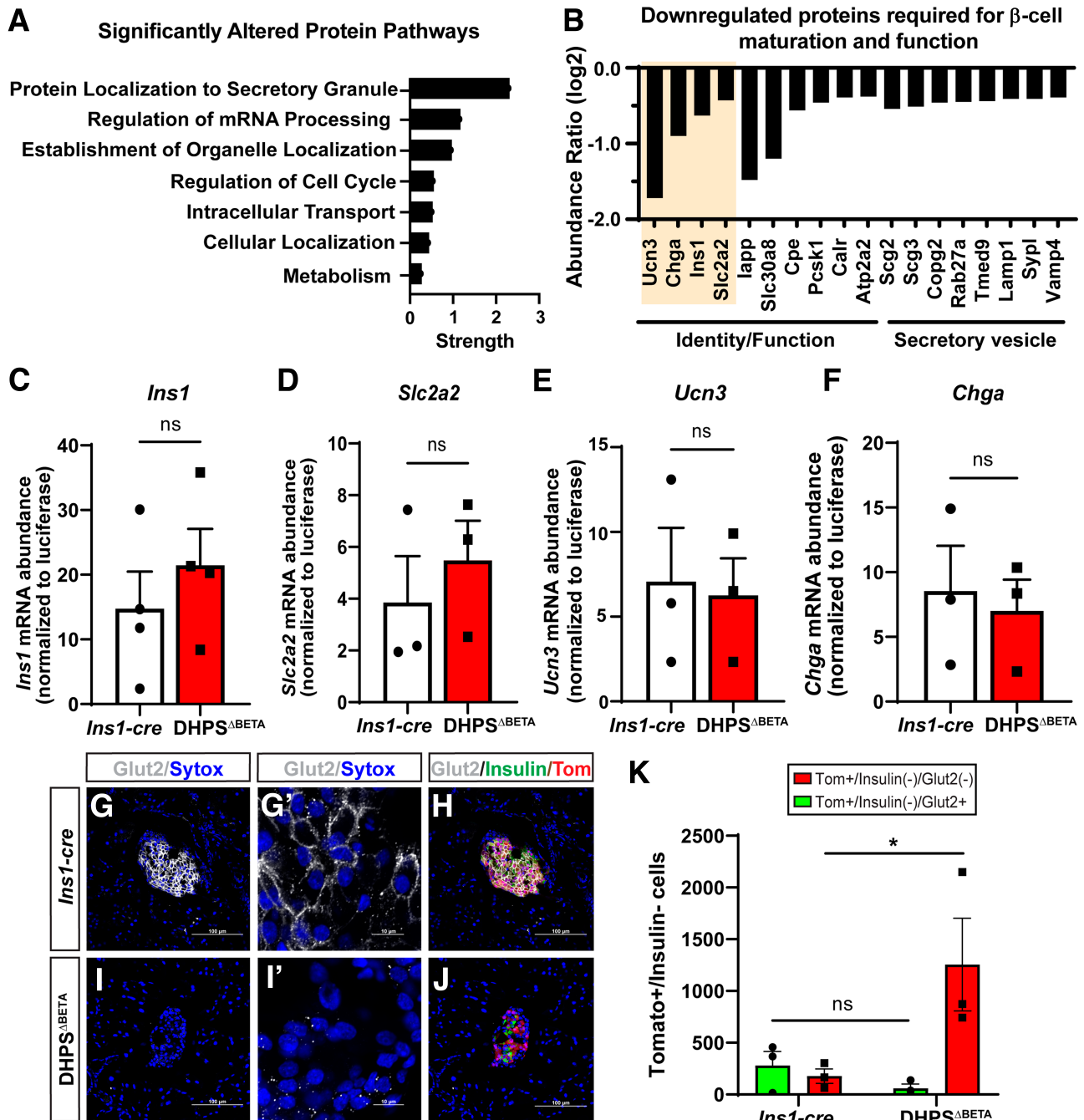


**Figure 5**—Islets from  $DHPS^{\Delta BETA}$  mice show altered protein synthesis and loss of identity in the  $\beta$ -cells. **A**: Pathway analysis performed on proteomic data from 4-week-old  $DHPS^{\Delta BETA}$  mutant islets compared with *Ins1-cre* controls. **B**: Select proteins from the pathway analysis are shown; these proteins required for  $\beta$ -cell maturation and function were downregulated in the 4-week-old  $DHPS^{\Delta BETA}$  mutant islets. The genes outlined by the shaded box were analyzed for transcript abundance. Real-time PCR was used to quantify gene expression of *Ins1* (**C**), *Slc2a2* (**D**), *Ucn3* (**E**), and *Chga* (**F**). Immunofluorescence was performed on pancreas tissue from 6-week-old *Ins1-cre* (**G** and **H**) and  $DHPS^{\Delta BETA}$  (**I** and **J**) mice to determine the coexpression of Glut2 (white) and insulin with the *R26R<sup>Tomato</sup>*  $\beta$ -cell lineage reporter (Tomato). Scale bar: 100  $\mu$ m. **G'** and **I'**: Localization of Glut2 (white) relative to nuclei marker (Sytox). Scale bar: 10  $\mu$ m. **K**: Tomato<sup>+</sup>/insulin<sup>-</sup>/Glut2<sup>-</sup> and Tomato<sup>+</sup>/insulin<sup>-</sup>/Glut2<sup>+</sup> cell populations were quantified ( $n = 3$ /group). Data are represented as mean  $\pm$  SEM. ns, not significant; \* $P < 0.05$ .

provided by  $DHPS/eIF5A^{HYP}$  in the early stages of  $\beta$ -cell differentiation and expansion. However, under circumstances of cellular stress, such as a rapid change in nutrition or increased metabolic load,  $eIF5A^{HYP}$  facilitates a critically important increased rate of protein synthesis. In

particular, we showed that in the absence of  $DHPS$ ,  $eIF5A$  is not activated via hypusination, resulting in a reduction in synthesis of specific proteins, including insulin and Glut2, which are needed for  $\beta$ -cells to mature and respond properly to new metabolic cues. It is clear from our

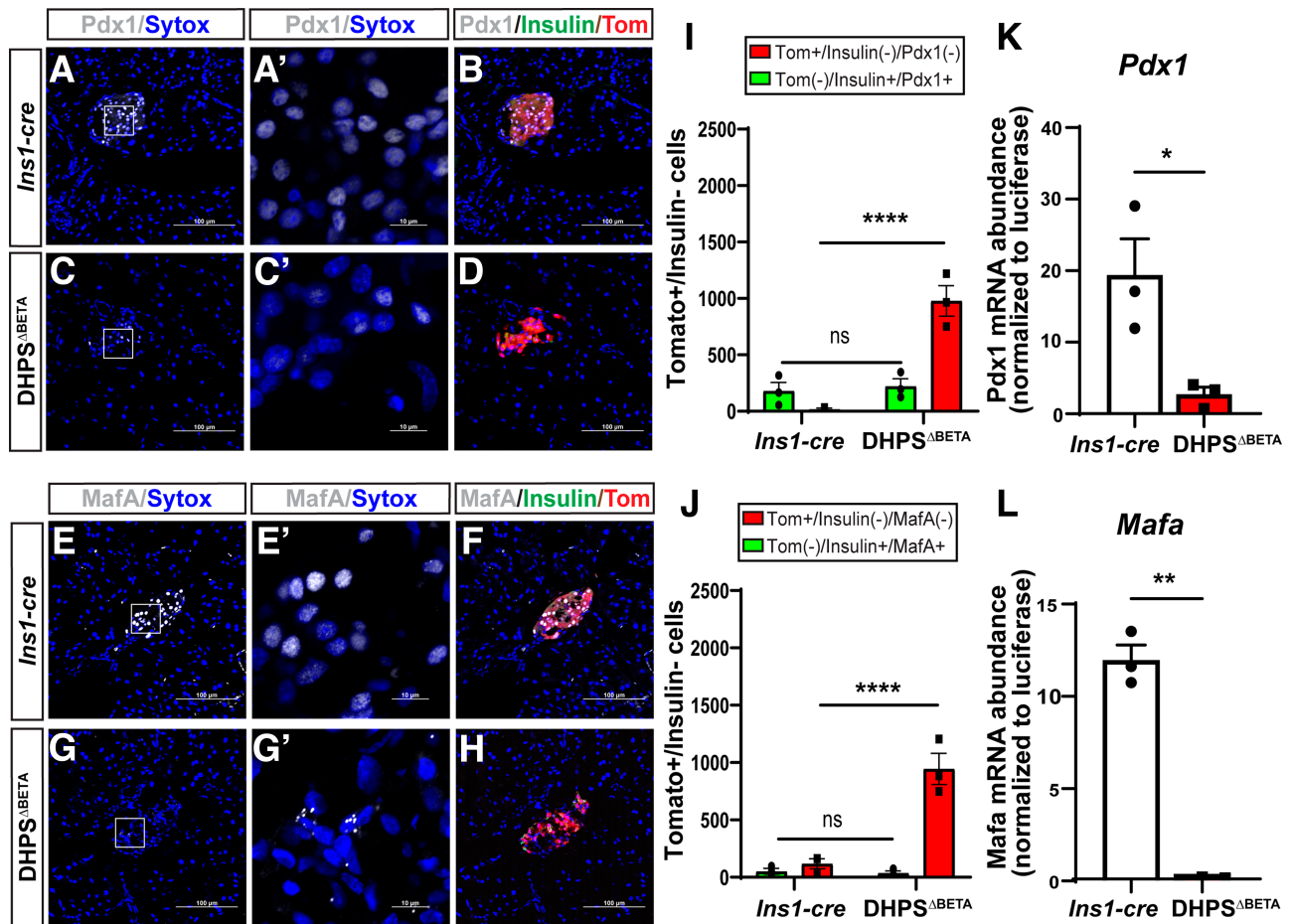


**Figure 6**—Markers of  $\beta$ -cell identity and function are reduced in  $DHPS^{\Delta BETA}$  islets. Immunofluorescence on pancreas tissue from 6-week-old *Ins1-cre* (A and B) and  $DHPS^{\Delta BETA}$  (C and D) mice to determine expression of insulin, the  $R26R^{Tomato}$   $\beta$ -cell lineage reporter (Tomato), and Pdx1 (white). Scale bar: 100  $\mu$ m. A' and C': Higher magnification to visualize localization of Pdx1. Scale bar: 10  $\mu$ m. Pancreas tissue from 6-week-old *Ins1-cre* (E and F) and  $DHPS^{\Delta BETA}$  (G and H) mice stained for insulin, Tomato, and MafA (white). Scale bar: 100  $\mu$ m. E' and G': Higher magnification to visualize localization of MafA. Scale bar: 10  $\mu$ m. I: Quantification of insulin deficient/lineage-labeled cells with or without Pdx1 expression. J: Quantification of insulin deficient/lineage-labeled cells with or without MafA expression. K: Transcript abundance of *Pdx1* normalized to *Luciferase* spike-in control gene expression. L: Transcript abundance of *Mafa* normalized to *Luciferase* spike-in control gene expression. Data are represented as mean  $\pm$  SEM ( $n = 3$ /group). ns, not significant \* $P < 0.05$ , \*\* $P < 0.01$ , \*\*\*\* $P < 0.0001$ .

previous (28) and current work that  $eIF5A^{HYP}$  is needed for the translation of only a subset of transcripts in certain cell types and at specific times, with the greatest induction of  $eIF5A^{HYP}$  being in response to stress.

As a secondary effect of reduced insulin and Glut2 synthesis and thus loss of  $\beta$ -cell functional identity, we observed loss of gene and protein expression of other  $\beta$ -cell identity markers, namely Pdx1 and MafA. Pdx1 abundance in  $\beta$ -cells has been shown to be regulated by glucose levels (44). Specifically, in the setting of low glucose, an increase in Pdx1 phosphorylation was observed, which marked Pdx1 for degradation (44). We therefore speculate that losing proper glucose signaling in the  $\beta$ -cells of  $DHPS^{\Delta BETA}$  mice due to reduced synthesis of insulin and Glut2 could signal the degradation of Pdx1. Similar to Pdx1, MafA expression was also previously shown to be regulated by glucose in  $\beta$ -cells, such that the transcript and protein levels of MafA depend on the concentration

of glucose (45). Altogether, we propose that the loss of  $eIF5A^{HYP}$  results in dysregulated translation of proteins critical for  $\beta$ -cell function, and as a result, there is a secondary loss of transcription factors that also function to maintain  $\beta$ -cell identity, which together culminates in a halting of  $\beta$ -cell maturation and the resultant onset of diabetes.

In mice,  $\beta$ -cell maturation occurs around weaning age, when the animals shift from a fat-rich milk diet to that of a carbohydrate-rich diet (12). Resultantly, the  $\beta$ -cells must rapidly acquire the machinery to respond to these new metabolic cues, which is a form of cellular stress. We propose that the  $\beta$ -cell has developed a translational regulatory mechanism that uses  $DHPS/eIF5A^{HYP}$  to increase the rate at which proteins critical for the  $\beta$ -cell secretory function must be synthesized to permit the  $\beta$ -cell to respond appropriately to new metabolic cues. Previously published work that investigated the role of *Dhps* in the

adult  $\beta$ -cell in the setting of a high-fat diet supports our conclusion that DHPS/eIF5A<sup>HYP</sup> is needed to regulate protein synthesis in the  $\beta$ -cell on demand (30). Our study determined that when the metabolic stress at weaning occurs, which requires the  $\beta$ -cell to increase the synthesis of certain proteins for functional maturation, the  $\beta$ -cell cannot mature without DHPS/eIF5A<sup>HYP</sup> and resultantly becomes dysfunctional. Levasseur et al. (30) conditionally deleted *Dhps* later in the life of the  $\beta$ -cell (8 weeks of age) and then provided the metabolic stress of a high-fat diet, which resulted in an inability of the  $\beta$ -cells to undergo compensatory proliferation in response to the demand. Although the context was different, the ultimate conclusion was the same, such that when a  $\beta$ -cell is placed in a setting that requires increased protein synthesis in response to demand (i.e., functional maturation at weaning or proliferation in response to a high-fat diet), DHPS/eIF5A<sup>HYP</sup> is needed to facilitate increased translation. In fact, the pathways affected in the mutant  $\beta$ -cells in both studies included metabolism, protein transport and mRNA processing/translation, which demonstrates that the loss of eIF5A<sup>HYP</sup> affects processes involved in  $\beta$ -cell response to stress. Furthermore, if one considers the studies investigating DHPS/eIF5A<sup>HYP</sup> in the exocrine pancreas (28,29), brain (46,47), and  $\beta$ -cell (30), and this study, we can see a common theme that suggests eIF5A<sup>HYP</sup> is a gatekeeper of specialized translation that permits professional secretory cells (exocrine, endocrine, neuron) to maintain their functional capacity during times of stress. In fact, perhaps all metabolically responsive secretory cells require a specialized translation factor to facilitate the integrity of specific protein production during times of induced/increased demand.

Studies in yeast support this idea that eIF5A<sup>HYP</sup> is required to increase the rate of read-through translation elongation for certain transcripts and that losing the activation of this specialized translation factor reduces the rate of protein synthesis but does not halt global translation (23). In this simplest eukaryotic organism, challenging sequences encoding stretches of consecutive amino acids, such as proline, require eIF5A<sup>HYP</sup> for efficient translation elongation (22,26). Further investigation is required to determine whether there are sequences within certain  $\beta$ -cell genes that specifically draw the function of eIF5A<sup>HYP</sup>. It is also critical to understand whether the eIF5A<sup>HYP</sup>-dependent translational regulatory mechanism plays a role in response to oxidative stress in the  $\beta$ -cell or the protection against diabetic  $\beta$ -cell failure in the setting of T1D, as both of these cellular contexts have been linked to altered protein synthesis (48–51). Altogether, it would be exciting to speculate that enhancing or restoring mRNA translation during periods of metabolic stress could maintain  $\beta$ -cell identity and function. Perhaps pharmacologically assisting the  $\beta$ -cell to increase protein synthesis during these times of excessive metabolic load could extend the ability of an ailing  $\beta$ -cell to maintain its functional maturation state and stave off the onset of diabetes.

In short, our mouse model has revealed a regulatory mechanism driven by DHPS/eIF5A<sup>HYP</sup> that is essential for metabolic health and  $\beta$ -cell function. It is well documented that  $\beta$ -cell dedifferentiation and dysfunction are hallmarks of diabetes pathogenesis (52,53). Understanding the mechanisms that impart  $\beta$ -cell identity could greatly assist the development of therapeutics to reestablish functional maturation in  $\beta$ -cells during the early stages of disease.

**Funding.** This work was supported by funding to T.L.M. from the JDRF (5-CDA-2016-194-A-N) and the National Institutes of Health (NIH), National Institute of Diabetes and Digestive and Kidney Diseases (R01DK121987), funding to C.B.P.V. from the Diabetes Research Connection (DRC56), and funding to S.R.R. from the NIH National Cancer Institute–Immuno-Oncology Translational Network: Data Management and Resource-Sharing Center (U24CA232979). The mass spectrometry work was performed by the Indiana University School of Medicine Center for Proteome Analysis and acquisition of the Indiana University School of Medicine Proteomics instrumentation was provided by the Indiana University Precision Health Initiative, which was supported, in part, by the Indiana Clinical and Translational Sciences Institute funded in part by the NIH, National Center for Advancing Translational Sciences, Clinical funds (UL1TR002529) and Translational Sciences Award, and the Cancer Center Support Grant for the Indiana University Simon Comprehensive Cancer Center from the National Cancer Institute (P30CA082709).

**Duality of Interest.** No potential conflicts of interest relevant to this article were reported.

**Author Contributions.** C.T.C., C.B.P.V., E.K.A.-B., S.R.R., C.D.R., P.J.C., L.R.P., M.A.R., and T.L.M. performed the research. C.T.C., C.B.P.V., E.K.A.-B., S.R.R., C.D.R., L.R.P., M.A.R., and T.L.M. analyzed data. C.T.C., C.B.P.V., E.K.A.-B., and T.L.M. wrote the paper. T.L.M. designed the study. All authors edited and approved the final draft of the manuscript. T.L.M. is the guarantor of this work and, as such, had full access to all the data in the study and takes responsibility for the integrity of the data and the accuracy of the data analysis.

## References

1. Fu Z, Gilbert ER, Liu D. Regulation of insulin synthesis and secretion and pancreatic Beta-cell dysfunction in diabetes. *Curr Diabetes Rev* 2013;9:25–53
2. MacDonald PE, Rorsman P. The ins and outs of secretion from pancreatic  $\beta$ -cells: control of single-vesicle exo- and endocytosis. *Physiology (Bethesda)* 2007;22:113–121
3. Kotzaeridou U, Young-Baird SK, Suckow V, et al. Novel pathogenic EIF2S3 missense variants causing clinically variable MEHMO syndrome with impaired eIF2 $\gamma$  translational function, and literature review. *Clin Genet* 2020;98:507–514
4. Parreiras-e-Silva LT, Luchessi AD, Reis RI, et al. Evidences of a role for eukaryotic translation initiation factor 5A (eIF5A) in mouse embryogenesis and cell differentiation. *J Cell Physiol* 2010;225:500–505
5. Pan FC, Wright C. Pancreas organogenesis: from bud to plexus to gland. *Dev Dyn* 2011;240:530–565
6. Jain C, Ansarullah, Bilekova S, Lickert H. Targeting pancreatic  $\beta$  cells for diabetes treatment. *Nat Metab* 2022;4:1097–1108
7. Ackermann AM, Gannon M. Molecular regulation of pancreatic  $\beta$ -cell mass development, maintenance, and expansion. *J Mol Endocrinol* 2007;38:193–206
8. Salinno C, Cota P, Bastidas-Ponce A, Tarquis-Medina M, Lickert H, Bakhti M.  $\beta$ -cell maturation and identity in health and disease. *Int J Mol Sci* 2019;20:5417
9. Bader E, Migliorini A, Gegg M, et al. Identification of proliferative and mature  $\beta$ -cells in the islets of Langerhans. *Nature* 2016;535:430–434
10. Blum B, Hrvatin S, Schuetz C, Bonal C, Rezanja A, Melton DA. Functional beta-cell maturation is marked by an increased glucose threshold and by expression of urocortin 3. *Nat Biotechnol* 2012;30:261–264

11. Zhang C, Moriguchi T, Kajihara M, et al. MafA is a key regulator of glucose-stimulated insulin secretion. *Mol Cell Biol* 2005;25:4969–4976
12. Stolovich-Rain M, Enk J, Vikesa J, et al. Weaning triggers a maturation step of pancreatic  $\beta$  cells. *Dev Cell* 2015;32:535–545
13. Park MH, Nishimura K, Zanelli CF, Valentini SR. Functional significance of eIF5A and its hypusine modification in eukaryotes. *Amino Acids* 2010;38:491–500
14. Park MH, Kar RK, Banka S, Ziegler A, Chung WK. Post-translational formation of hypusine in eIF5A: implications in human neurodevelopment. *Amino Acids* 2022;54:485–499
15. Davies JL, Kawaguchi Y, Bennett ST, et al. A genome-wide search for human type 1 diabetes susceptibility genes. *Nature* 1994;371:130–136
16. Grattan M, Mi QS, Meagher C, Delovitch TL. Congenic mapping of the diabetogenic locus *Idd4* to a 5.2-cM region of chromosome 11 in NOD mice: identification of two potential candidate subloci. *Diabetes* 2002;51:215–223
17. Mastracci TL, Colvin SC, Padgett LR, Mirmira RG. Hypusinated eIF5A is expressed in the pancreas and spleen of individuals with type 1 and type 2 diabetes. *PLoS One* 2020;15:e0230627
18. Maier B, Ogihara T, Trace AP, et al. The unique hypusine modification of eIF5A promotes islet  $\beta$  cell inflammation and dysfunction in mice. *J Clin Invest* 2010;120:2156–2170
19. Park MH. The post-translational synthesis of a polyamine-derived amino acid, hypusine, in the eukaryotic translation initiation factor 5A (eIF5A). *J Biochem* 2006;139:161–169
20. Park MH. Regulation of biosynthesis of hypusine in Chinese hamster ovary cells. Evidence for eIF-4D precursor polypeptides. *J Biol Chem* 1987;262:12730–12734
21. Park MH, Wolff EC, Smit-McBride Z, Hershey JW, Folk JE. Comparison of the activities of variant forms of eIF-4D. The requirement for hypusine or deoxyhypusine. *J Biol Chem* 1991;266:7988–7994
22. Pelechano V, Alepuz P. eIF5A facilitates translation termination globally and promotes the elongation of many non polyproline-specific tripeptide sequences. *Nucleic Acids Res* 2017;45:7326–7338
23. Saini P, Eyler DE, Green R, Dever TE. Hypusine-containing protein eIF5A promotes translation elongation. *Nature* 2009;459:118–121
24. Dever TE, Green R. The elongation, termination, and recycling phases of translation in eukaryotes. *Cold Spring Harb Perspect Biol* 2012;4:a013706
25. Gregio AP, Cano VP, Avaca JS, Valentini SR, Zanelli CF. eIF5A has a function in the elongation step of translation in yeast. *Biochem Biophys Res Commun* 2009;380:785–790
26. Gutierrez E, Shin BS, Woolstenhulme CJ, et al. eIF5A promotes translation of polyproline motifs. *Mol Cell* 2013;51:35–45
27. Li CH, Ohn T, Ivanov P, Tisdale S, Anderson P. eIF5A promotes translation elongation, polysome disassembly and stress granule assembly. *PLoS One* 2010;5:e9942
28. Padgett LR, Robertson MA, Anderson-Baucum EK, et al. Deoxyhypusine synthase, an essential enzyme for hypusine biosynthesis, is required for proper exocrine pancreas development. *FASEB J* 2021;35:e21473
29. Mastracci TL, Robertson MA, Mirmira RG, Anderson RM. Polyamine biosynthesis is critical for growth and differentiation of the pancreas. *Sci Rep* 2015;5:13269
30. Levasseur EM, Yamada K, Piñeros AR, et al. Hypusine biosynthesis in  $\beta$  cells links polyamine metabolism to facultative cellular proliferation to maintain glucose homeostasis. *Sci Signal* 2019;12:eaax0715
31. Thorens B, Tarussio D, Maestro MA, Rovira M, Heikkilä E, Ferrer J. *Ins1(Cre)* knock-in mice for beta cell-specific gene recombination. *Diabetologia* 2015;58:558–565
32. Madisen L, Zwingman TA, Sunkin SM, et al. A robust and high-throughput Cre reporting and characterization system for the whole mouse brain. *Nat Neurosci* 2010;13:133–140
33. Mastracci TL, Anderson KR, Papizan JB, Sussel L. Regulation of Neurod1 contributes to the lineage potential of Neurogenin3+ endocrine precursor cells in the pancreas. *PLoS Genet* 2013;9:e1003278
34. Bankhead P, Loughrey MB, Fernández JA, et al. QuPath: open source software for digital pathology image analysis. *Sci Rep* 2017;7:16878
35. Lacy PE, Kostianovsky M. Method for the isolation of intact islets of Langerhans from the rat pancreas. *Diabetes* 1967;16:35–39
36. Szklarczyk D, Gable AL, Nastou KC, et al. The STRING database in 2021: customizable protein-protein networks, and functional characterization of user-uploaded gene/measurement sets. *Nucleic Acids Res* 2021;49:D605–D612
37. Kim JA, Vetrivel P, Kim SM, et al. Quantitative proteomics analysis for the identification of differential protein expression in calf muscles between young and old SD rats using mass spectrometry. *ACS Omega* 2021;6:7422–7433
38. Slenter DN, Kutmon M, Hanspers K, et al. WikiPathways: a multifaceted pathway database bridging metabolomics to other omics research. *Nucleic Acids Res* 2018;46:D661–D667
39. Shannon P, Markiel A, Ozier O, et al. Cytoscape: a software environment for integrated models of biomolecular interaction networks. *Genome Res* 2003;13:2498–2504
40. Gutiérrez GD, Bender AS, Cirulli V, et al. Pancreatic  $\beta$  cell identity requires continual repression of non- $\beta$  cell programs. *J Clin Invest* 2017;127:244–259
41. Finegood DT, Scaglia L, Bonner-Weir S. Dynamics of  $\beta$ -cell mass in the growing rat pancreas. Estimation with a simple mathematical model. *Diabetes* 1995;44:249–256
42. Dor Y, Brown J, Martinez OI, Melton DA. Adult pancreatic  $\beta$ -cells are formed by self-duplication rather than stem-cell differentiation. *Nature* 2004;429:41–46
43. Bouwens L, Rooman I. Regulation of pancreatic beta-cell mass. *Physiol Rev* 2005;85:1255–1270
44. Humphrey RK, Yu SM, Flores LE, Jhala US. Glucose regulates steady-state levels of PDX1 via the reciprocal actions of GSK3 and AKT kinases. *J Biol Chem* 2010;285:3406–3416
45. Kataoka K, Han SI, Shioda S, Hirai M, Nishizawa M, Handa H. MafA is a glucose-regulated and pancreatic  $\beta$ -cell-specific transcriptional activator for the insulin gene. *J Biol Chem* 2002;277:49903–49910
46. Kar RK, Hanner AS, Starost MF, et al. Neuron-specific ablation of eIF5A or deoxyhypusine synthase leads to impairments in growth, viability, neurodevelopment, and cognitive functions in mice. *J Biol Chem* 2021;297:101333
47. Padgett LR, Shinkle MR, Rosario S, et al. Deoxyhypusine synthase mutations alter the post-translational modification of eukaryotic initiation factor 5A resulting in impaired human and mouse neural homeostasis. *HGG Adv* 2023;4:100206
48. Good AL, Haemmerle MW, Oguh AU, Doliba NM, Stoffers DA. Metabolic stress activates an ERK/hnRNPK/DDX3X pathway in pancreatic  $\beta$  cells. *Mol Metab* 2019;26:45–56
49. Good AL, Cannon CE, Haemmerle MW, et al. JUND regulates pancreatic  $\beta$  cell survival during metabolic stress. *Mol Metab* 2019;25:95–106
50. Lee K, Chan JY, Liang C, et al. XBP1 maintains beta cell identity, represses beta-to-alpha cell transdifferentiation and protects against diabetic beta cell failure during metabolic stress in mice. *Diabetologia* 2022;65:984–996
51. Engin F. ER stress and development of type 1 diabetes. *J Investig Med* 2016;64:2–6
52. Accili D, Talchai SC, Kim-Muller JY, et al. When  $\beta$ -cells fail: lessons from dedifferentiation. *Diabetes Obes Metab* 2016;18(Suppl. 1):117–122
53. Cinti F, Bouchi R, Kim-Muller JY, et al. Evidence of  $\beta$ -cell dedifferentiation in human type 2 diabetes. *J Clin Endocrinol Metab* 2016;101:1044–1054